Journal of Institute of Science and Technology, 31(1), 159-170 (2026)
ISSN: 2467-9062 (print), e-ISSN: 2467-9240
https://doi.org/10.3126/jist.v31i1.86813

Research Article

VALORIZATION OF WASTE MAIZE COBS AS A LOW-COST ADSORBENT FOR ARSENIC (III) REMOVAL FROM WATER

Bhoj Raj Poudel[1], Sabin Dhungana[2], Krishna Subedi[2,3], Devendra Khadka[2,4], Hari Paudyal[2*], Megh Raj Pokhrel[2]

[1]*Department of Chemistry, Tri-Chandra Multiple Campus, Tribhuvan University, Kathmandu, Nepal*
[2]*Central Department of Chemistry, Tribhuvan University, Kirtipur, Kathmandu, Nepal*
[3]*Department of Chemistry, Donaghey College of Science, Technology, Engineering and Mathematics, University of Arkansas at Little Rock, Little Rock, USA*
[4]*Department of Chemistry, Tribhuvan Multiple Campus, Tribhuvan University, Tansen, Palpa, Nepal*
**Correspondence: haripaudyal9@gmail.com*

(*Received*: November 24, 2025; *Revised*: January 6, 2026; *Accepted*: June 7, 2026)

ABSTRACT

The toxicity of arsenic has drawn a lot of attention to its presence in groundwater resources. In this study, As(III) was removed from aqueous solution using Zr(IV)-loaded modified maize cob (Zr(IV)-MMC). FTIR and XRD analysis confirmed effective modification of maize cob, whereas SEM images revealed surface roughening after Zr loading and EDX confirmed that As(III) was adsorbed onto Zr(IV)-MMC. Zr(IV)-MMC showed a good adsorption capacity (q_{max} = 43.26 mg/g, pH = 9.0), and with 2M NaOH, the desorption rate could reach 95.24%, making it a promising regenerable adsorbent. The Langmuir isotherm and pseudo-second order (PSO) kinetics models provided a good fit to the experimental data. The adsorption of As(III) onto Zr(IV)-MMC was most interfered with by phosphate out of the co-existing ions: sulphate, phosphate, chloride, and nitrate. For the desorption of adsorbed As(III) for regeneration, a 2M NaOH solution proved to be an efficient eluent. This study shows that the low-cost Zr(IV)-MMC adsorbent is an economical, eco-friendly, and effective adsorbent that not only safely eliminates As(III) from water but also enables recycling and reuse of the biowaste.

Keywords: Adsorption, Adsorption capacity, Arsenite, Maize cobs, Zr(IV)-loading

INTRODUCTION

Arsenic is a widespread element in the Earth's crust that naturally occurs in soil and water from rock leaching, in addition to human actions including mining, burning fossil fuels, and spraying pesticides (Aryal et al., 2010). As(III) can exist in aquatic systems in oxidation states of -3, 0, +3, and +5, and it is more hazardous than As(V) and organic arsenicals (Thapa & Pokhrel, 2013). Arsenate [As(V)] and arsenite [As(III)] are the stable dissolved species, with $H_2AsO_4^-$ dominant at pH 3–7 and $HAsO_4^{2-}$ at pH 7–11 in oxidized waters. When reducing circumstances are present, neutral H_3AsO_3 is dominant. The WHO has established a limit of 10 µg/L for arsenic in drinking water, but China, Bangladesh, and Nepal have a preliminary guideline of 50 µg/L (Chand et al., 2015).

Ion exchange, oxidation with ozone and chlorine, lime treatment, adsorption, co-precipitation with iron or alum, membrane processes like reverse osmosis, and technologies involving plants and microbes are some of the most widely used technologies of interest (Singh et al., 2021). Adsorbents play a key role in adsorption, which is one of these simple, economical, and environmentally friendly wastewater treatment techniques. Research aims to create low-cost, non-toxic, and efficient adsorbents, such as agricultural waste, which is abundant in functional groups (Luo et al., 2017).

Various bioadsorbents have been developed for As(III) and As(V) removal. Amin et al. (2006) reported that raw rice husk removed arsenic at 100 µg/L using an adsorption column, achieving 96% desorption efficiency with 1M KOH. Chemically modified maize cobs showed 98% arsenite removal efficiency at 50 mg/mL (Elizalde-González et al., 2008), whereas Fe(III)-loaded *Staphylococcus xylosus* biomass adsorbed 54.35 mg As(III) at pH 7 and 61.34 mg As(V) at pH 3 (Aryal et al., 2010). Fe(III)-loaded charred pomegranate had a maximum As(III) adsorption of 50 mg/g at pH 9 (Thapa & Pokhrel, 2013). Using Fe(III)-loaded sugarcane bagasse, Chand et al. (2015) achieved maximum adsorption of 25 mg/g As(III) at pH 8 and 70 mg/g As(V) at pH 5, with data that suit the Langmuir isotherm and pseudo second order (PSO) models.

According to Montero et al. (2018), Fe-modified biochar derived from sugarcane bagasse and maize cob husk outperformed activated carbon in removing 85–99.9% of As(III) from 1000 µg/L solutions.

Maize cobs (MC) contain high lignocellulose with hydroxyl groups, offering hydrophilicity and biodegradability, making them advantageous for adsorption. For instance, hexavalent chromium has been extracted from water using polyethyleneimine-functionalized maize cob, utilizing the idea of "using waste to treat waste" (Xu et al., 2022). Maize cobs are rich in lignocellulosic components, primarily cellulose, hemicellulose and lignin along with pectin, soluble extractives (fats and waxes), and ash. The pectin surrounds the fibres, giving maize cobs a sheet-like structure (Yang & Zhou, 2012). However, untreated MC surfaces have few active adsorption sites, which results in a low adsorption amount and a lack of selectivity (Luo et al., 2017). In addition to this, Zr-based compounds have higher adsorption capacity for arsenic, possibly due to the strong Lewis acid-base interaction, particularly between As(V) and Zr-OH groups (Paz et al., 2022).

Although several agricultural wastes have been modified using lime and Zr(IV) for arsenic removal, no study has reported the synthesis or application of Zr(IV)-loaded NaOH modified maize cobs**.** The present work introduces a two-step modification strategy involving (i) alkali treatment of maize cobs to enrich carboxylate functional groups and (ii) subsequent Zr(IV) loading to create anion exchange site. This integrated modification pathway has not been explored previously for maize-cob-based adsorbents. Thus, this study fills a critical research gap by offering a novel, low-cost, and mechanistically distinct Zr(IV)-loaded alkali modified maize cob adsorbent for efficient As(III) remediation. The efficiency of this adsorbent in removing arsenite from aqueous solutions was evaluated through batch adsorption experiments because no research has been published on Zr(IV)-loaded NaOH modified maize cobs. Additionally, the adsorption isotherm and kinetic characteristics were assessed. Moreover, the effect of interfering ions as well as the desorption of the arsenite for recycling of the adsorbent was also studied.

MATERIALS AND METHODS

Materials

Analytical grade reagents were used; no further purification was performed on them. Sodium arsenite was from S.D. Fine Chemicals with 99% purity. Ammonium heptamolybdate, hydrazine hydrate, potassium permanganate, sulphuric acid, hydrochloric acid, sodium hydroxide, oxalic acid, and buffer tablets were sourced from Qualigens Fine Chemicals, exhibiting a purity range of 97% to 99.5%. All other chemicals were from Thermo Fisher Scientific with a purity of 99%. A 1000 mg/L stock solution of As(III) was prepared by dissolving an appropriate amount of sodium arsenite ($NaAsO_2$) in deionized water. Working solutions of desired concentrations were prepared by appropriate dilution of the stock solution with deionized water immediately before use.

Preparation of the adsorbent

Adsorbent was synthesized using a slightly modified method as described by Biswas et al. (2008). Maize Cobs were collected from Hetauda, Makawanpur. The low-cost adsorbent was prepared through sequential crushing, pulverization, sieving, and chemical modification, making it economical and readily available material for water treatment. The efficiency of this adsorbent in extracting arsenite from aqueous solution was produced and investigated. After being cleaned with distilled water until it was clear, at 65 °C, the biomass was dried for 24 hours. and then pulverized to give fine powder and stored in an airtight plastic bottle, which is known as raw maize cobs (RMC). For Zr(IV)-MMC preparation, 20 g of RMC was first immersed in 0.1 M NaOH (400 mL) at 190 rpm and 298 K for 24 hours, then filtered, washed to neutral pH, and dried at 65 °C. The resulting material is known as modified maize cob (MMC), and Zr(IV) was loaded in the following manner. Ten grams of MMC were treated with 0.1M Zr(IV) solution and shaken for 24 hours. Thereafter, it was filtered, cleaned until neutral pH and dried at 65 °C, yielding Zr(IV)-loaded modified maize cobs, which are abbreviated as Zr(IV)-MMC.

Characterization

The biosorbent was characterized using FTIR, XRD, and SEM analyses. FTIR spectroscopy was performed using a PerkinElmer Spectrum IR (version 10.6.2) to analyze the functional groups in adsorbents. A Rigaku diffractometer (Japan) equipped with Cu Kα radiation (λ = 1.54056 Å) was used for XRD examination to assess the crystallinity of the bio-adsorbent. To analyse the material's surface morphology, a field-emission scanning electron microscope (FE-SEM; JEOL JSM-6701F, Japan) was used.

Batch adsorption study

The percentage adsorption (%) and adsorption capacity (mg/g) at equilibrium were computed using the subsequent formula:

$$\%A = \frac{C_i - C_e}{C_i} \times 100 \quad \ldots (1)$$

$$q = \frac{C_i - C_e}{W} \times V \quad \ldots (2)$$

where C_i represents the adsorbate solution's starting concentration and C_e represents its equilibrium concentration (mg/L). W stands for the weight of the adsorbent (g) and V for the volume of arsenic solution (L) in the adsorption tests.

The concentration of As(III) in aqueous solutions was determined using the arsenomolybdenum blue method according to the American Public Health Association (APHA, 2017). In brief, an aliquot of the sample was treated with ammonium molybdate under acidic conditions to form the arsenomolybdate complex, which was then reduced to a blue-colored arsenomolybdenum complex using stannous chloride. The intensity of the blue color was measured spectrophotometrically at λ_{max} = 860 nm using a UV-Visible double beam spectrophotometer (Labtronics, LT-2802, India). Calibration curves were prepared with standard As(III) solutions, and all measurements were performed in triplicate. Potential interferences from phosphate and silicate were minimized by maintaining acidic conditions during the color development.

RESULTS AND DISCUSSION

Characterization of the adsorbent

Figure 1(a) displays the key functional groups' FTIR spectra. The wide band at 3300–3400 cm^{-1} is associated with -NH_2 groups and O–H stretching in cellulose, pectin, and lignin, which shifts to 3330 and 3340 cm^{-1}, indicating interactions with zirconium and arsenic oxides (Biswas et al., 2008; Sheng et al., 2014; Lin et al., 2018). The weak C–H stretching band at 2970 cm^{-1} shifts to 2939 and 2900 cm^{-1} after Zr(IV) loading and As(III) adsorption, suggesting loss of aliphatic wax fractions (Biswas et al., 2008). The FTIR absorption bands observed in the 2000–2500 cm^{-1} region were assigned to the stretching vibrations of C≡C and C≡N functional groups, consistent with previous reports (Samsuri et al., 2013). Key adsorption-related shifts occur in the 1200–1800 cm^{-1} range. Absorption peaks in 1700–1900 cm^{-1} (C=O) and 1600–1700 cm^{-1} (C–O) signify the participation of adsorption. The carboxyl group peaks at 1600 cm^{-1} and 1460 cm^{-1} shifts to 1635/1420 cm^{-1} (Zr(IV)-MMC), confirming adsorption. A peak corresponding to aromatic C=C stretching is located at 1512 cm^{-1}. Absorption peaks at 1300–1000 cm^{-1} indicate C–O stretching in carboxylic acids, alcohols, and ethers (Baig et al., 2009). Upon metal binding, the 1033 cm^{-1} peak, representing C–O stretching, and the 1234 cm^{-1} peak, representing carboxyl C–O stretch, undergo a shift. Additional peaks at 879 and 894 cm^{-1} are associated with stretching of Zr–O and As–O (Biswas et al., 2008; Baig et al., 2009; Samsuri et al., 2013). FTIR confirms that the bio-adsorbent surface is rich in polymeric hydroxyl and carboxylic groups, mainly from lignin and cellulose, which facilitate metal binding in aqueous solutions.

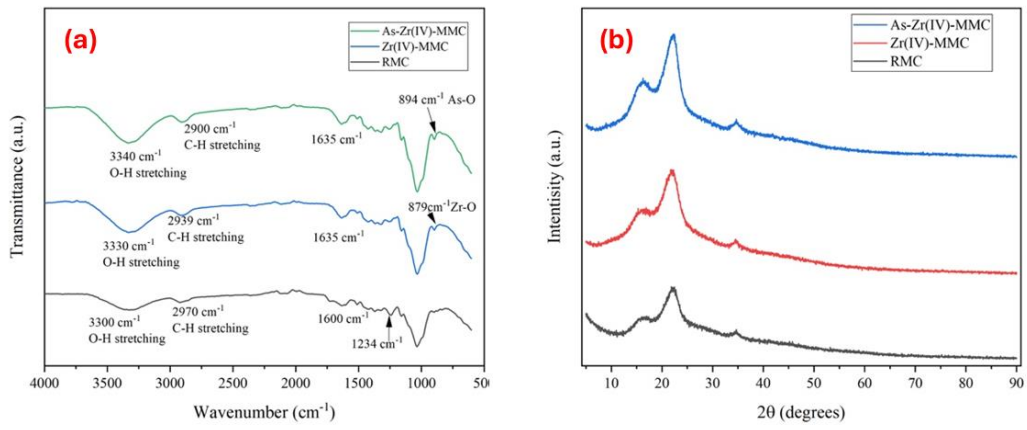

Figure 1. (a) FTIR spectrum of RMC, Zr(IV)-MMC and As(III)-Zr(IV)-MMC and (b) XRD plots of RMC, Zr(IV)-MMC and As-Zr(IV)-MMC

The XRD pattern in Figure 1(b) of RMC exhibits strong peaks at 2θ values of 18º and 22º, indicating the crystalline nature of cellulose, as well as faint, dispersed peaks at greater angles that represent its amorphous areas. This suggests that RMC comprises both crystalline and amorphous structures. The peak at 2θ = 22º remains unchanged in Zr(IV)-MMC and As(III)-Zr(IV)-MMC, signifying that modifications and adsorption occur mainly in the amorphous region. Additionally, peaks at approximately 34.50º correspond to amorphous ZrO_2 (Zong et al., 2013). Variations in the intensity of these peaks indicate changes due to the arsenic adsorption process.

SEM was used to observe the morphological properties of adsorbents. It was found that treatment of maize cobs with a base improved surface morphology. Figure 2a depicts that the SEM image of Zr(IV)-MMC possesses heterogeneous pores with irregular shapes. The porous structure enhanced the adsorbent's surface area, which is important for adsorption. The surface becomes somewhat smoother after As(III) adsorption in the case of As-Zr(IV)-MMC (Fig. 2b). It is reasonable to assume that this was caused by the filling of As(III) in the pores of Zr(IV)-MMC.

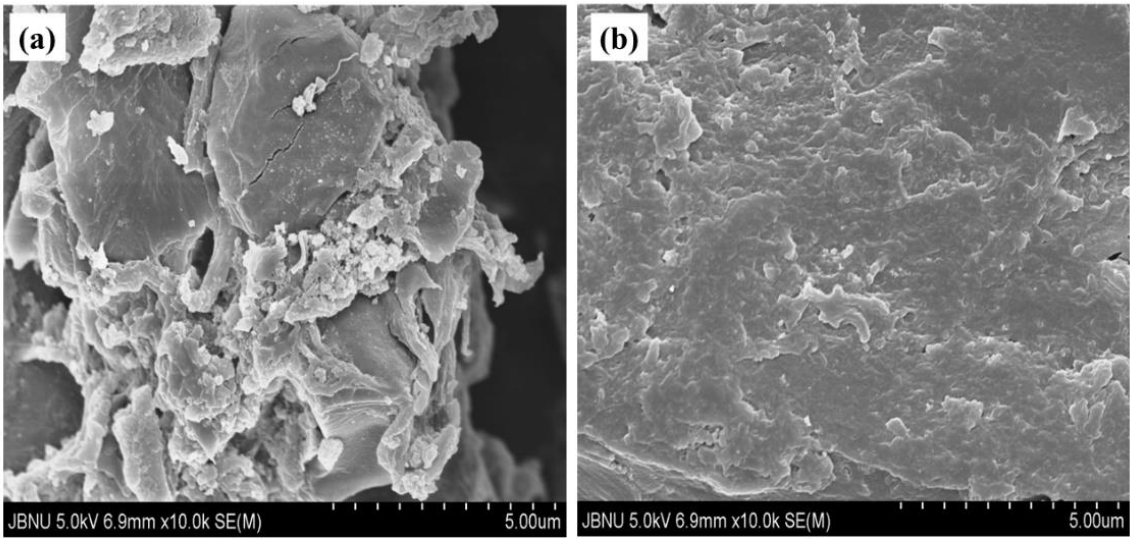

Figure 2. SEM images of adsorbents: (a) Zr(IV)-MMC, (b)As- Zr(IV)-MMC

Figure 3 revealed the EDX spectra of arsenic-adsorbed Zr(IV)-MMC. The elements C, O, Si, Zr, and As are represented by the peak in the EDX spectra of arsenic-adsorbed Zr(IV)-MMC. This indicates that As(III) was adsorbed onto the Zr(IV)-MMC.

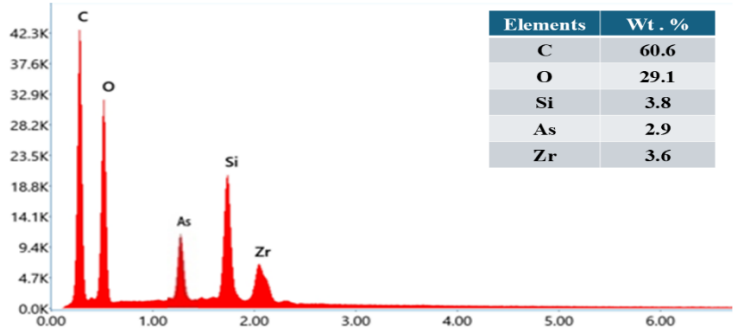

Elements	Wt . %
C	60.6
O	29.1
Si	3.8
As	2.9
Zr	3.6

Figure 3. EDX spectrum of arsenic-adsorbed Zr(IV)-MMC with a table showing elemental composition (in inset)

Effect of pH

Since pH controls whether the active site is protonated or deprotonated, it has a significant impact on the adsorbent's surface charge and the existence of active adsorption sites. Furthermore, arsenite can take on distinct forms based on the pH of the solution, acting as $H_2AsO_3^-$ in pH 8–12 and H_3AsO_3 in acidic pH. All of these factors cause the adsorption of As(III) to change as the pH of the solution changes (Pant et al., 2024).

The effect of pH on the adsorption of As(III) on RMC and Zr(IV)-MMC was examined by maintaining the solution's initial pH between 2 and 12. Figure 4 showed that for both RMC and Zr(IV)-MMC, the basic condition was favourable for adsorption. Both these adsorbents showed maximum adsorption at pH 9.0, which aligns well with the study carried out by Pant et al. (2024). As(III) *adsorption* increased under alkaline conditions, which can be explained by changes in arsenite speciation. At pH < 8, As(III) predominantly exists as the neutral species H_3AsO_3, which interacts mainly via ligand exchange with Zr(IV) centers. However, at pH values above 8, H_3AsO_3 increasingly deprotonates to form $H_2AsO_3^-$, which can be more strongly attracted to the partially positive Zr(IV) sites on the biosorbent surface. This enhances adsorption through a combination of electrostatic interactions and inner-sphere complexation. Because the anionic species of As(III) predominate at pH 8 to 10, the oxyanion of As(III) can exchange hydroxyl ions more favorably, increasing As(III) adsorption. As(III) biosorption decreased at higher pH (>10) due to competition between As(III) oxyanions and hydroxide ions. Previous studies also report similar behavior, where Zr-modified biomass exhibits high affinity for arsenite at alkaline pH due to strong ligand exchange mechanisms (Biswas et al., 2008; Poudel et al., 2022). However, the % adsorption in the case of RMC was not significant as compared to that of Zr(IV)-MMC (Fig.4a, 4b). So, further experiments were solely performed using the modified adsorbent.

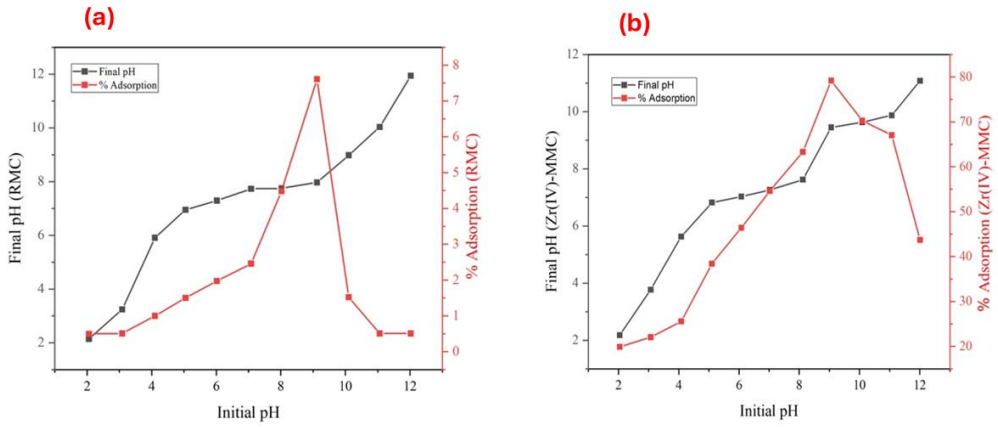

Figure 4. Plot of final pH and % adsorption against initial pH of the solution for (a) RMC and (b) Zr(IV)-MMC

Effect of contact time and adsorption kinetics

Both pseudo-first-order (PFO) and pseudo-second-order (PSO) models for As(III) adsorption onto Zr(IV)-MMC were investigated. The following is the non-linear equation for pseudo-first-order kinetics (Lagergren 1898):

$$q_t = q_e(1 - e^{-K_1 t}) \quad \ldots (3)$$

Similarly, the non-linear equation for PSO kinetics is as follows (Blanchard et al., 1984):

$$q_t = \frac{q_e^2 K_2 t}{1 + q_e K_2 t} \quad \ldots (4)$$

where q_e and q_t (mg/g) are the adsorption capacity at equilibrium and at time t, respectively; and k_1, (min^{-1}) and k_2 (g/mg min) are the rate constants of PFO and PSO kinetics, respectively.

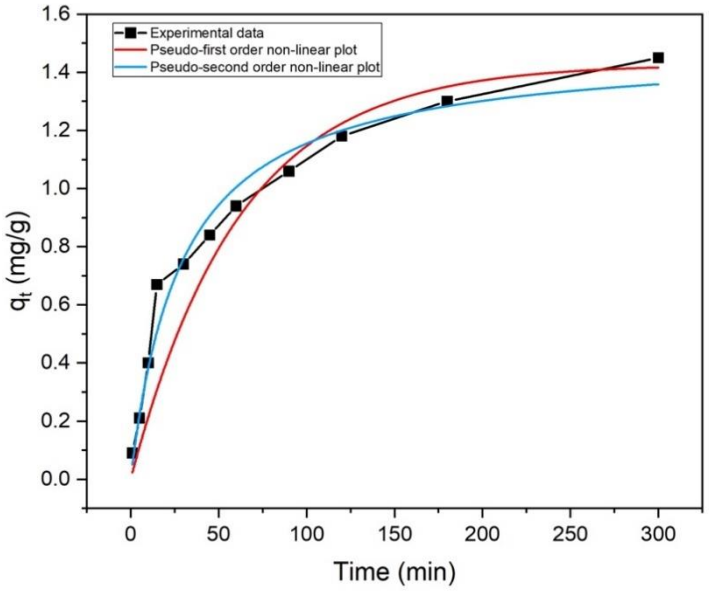

Figure 5. Non-linear fitting for models of PSO and PFO kinetics

The kinetic curve (Fig. 5) demonstrates that As(III) adsorption rises with time and reaches equilibrium after five hours. However, to ensure all the adsorption sites were occupied, the adsorption experiment was carried out for 24 hours and was maintained throughout the whole study. The PFO and PSO models' ability to fit the kinetic data is shown by the resulting graphs. However, the PSO model that best fits the adsorption data has a larger R^2 value, suggesting that PSO kinetics govern the adsorption of As(III) on Zr(IV)-MMC.

Table 1. Kinetic parameters established for the adsorption of As(III)

Adsorbent	**Exp. ($q_{eep.}$) (mg/g)**	**PFO model**			**PSO model**		
		k_1 (min^{-1})	q_e (mg/g)	R^2	k_2 (g/mg min)	q_e (mg/g)	R^2
Zr(IV)-MMC	1.650	0.028	1.279	0.865	0.0231	1.489	0.970

Adsorption isotherm

Monolayer adsorption is suggested by the Langmuir isotherm model when there is no observable interaction among the adsorbed species. Equations (5) and (6) reflect the Langmuir isotherm's linear and non-linear versions, respectively (Langmuir 1918):

$$\frac{C_e}{q_e} = \frac{1}{q_m b} + \frac{C_e}{q_m} \quad \ldots(5)$$

$$q_e = \frac{q_m b C_e}{1 + b C_e} \quad \ldots(6)$$

In this context, b represents the Langmuir constant, q_e denotes the equilibrium sorption capacity, q_m signifies the maximum adsorption capacity, and C_e indicates the equilibrium adsorbate concentration.

Similarly, the Freundlich isotherm implies multilayer adsorption, indicating possible interaction between the species adsorbed on a heterogeneous surface. The linear version of the Freundlich isotherm is seen in equation (7) (Freundlich, 1907).

$$\log q_e = \log K_F + \left(\frac{1}{n}\right) \log C_e \quad \ldots(7)$$

This equation transforms into a non-linear form as:

$$q_e = K_F(C_e)^{\frac{1}{n}} \quad \ldots(8)$$

where KF is the adsorption capacity-related Freundlich constant and,$1/n$. This heterogeneity factor has no dimensions.

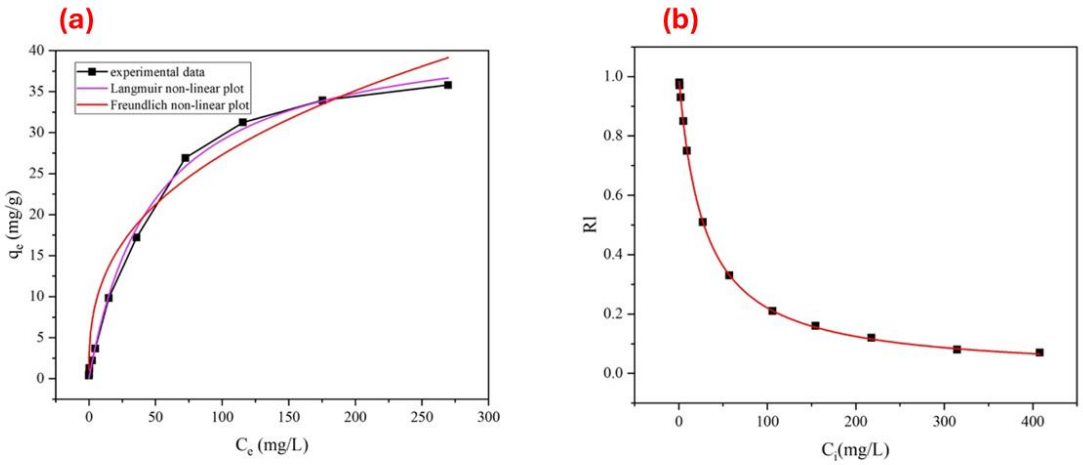

Figure 6. (a) Zr(IV)-MMC isotherm plot with non-linear fitting for the Freundlich and Langmuir isotherms, and (b) relationship between separation factor and initial concentration

Figure 6a show that both models produced linear plots, However, the linear plot of the Langmuir model fits the experimental data more accurately than the Freundlich model. This is indicated by the Langmuir model's higher correlation coefficient (R^2) value, which shows that the active sites are distributed uniformly and that adsorption is restricted to a monolayer only (Ho & McKay, 1998).

Table 2. Isotherms parameters for the biosorption of As(III)

Adsorbent	**Exp. q_{max} (mg/g)**	**Langmuir**			**Freundlich**		
		q_{max} (mg/g)	**b (L/mg)**	**R^2**	**K_F (L/g)**	**1/n**	**R^2**
Zr(IV)-MMC	41.94	43.26	0.020	0.997	5.124	0.363	0.959

In Figure 6b, the value of R_L ranges from 0 to 1, indicates that the equilibrium data are in good agreement with the Langmuir adsorption isotherm. On the other hand, the 1/n values from the Freundlich model, which similarly range from 0 to 1, indicate a favourable adsorption process. The maximal adsorption capacity for Zr(IV)-MMC, or q_{max}, is estimated by the Langmuir isotherm model to be 43.26 mg/g. The q_{max} value for the adsorbent closely aligns with the adsorption capacity derived from the plateau region of the isotherm curve, measured at 36.94 mg/g for Zr(IV)-MMC. Table 3 summarizes the comparison between the Zr(IV)-MMC adsorbent's maximal adsorption capacity and other bio-adsorbents for the removal of As(III) from water. This shows that Zr(IV)-loaded MMC can still be a better bio-adsorbent for sequestrating As(III) from aqueous solution.

Table 3. Comparison of q_{max} for As(III) removal from water using various adsorbents

S.N.	Adsorbent	Optimum pH	Temp. (K)	q_{max} (mg/g)	Reference
1	Maize cob husk Fe-coated biochars	4		50	Montero et al., 2018
2	La(III)- modified watermelon rind	12.08	298	37.73	Aryal et al., 2022
3	La(III)- modified watermelon rind	12.08	303	48.78	Aryal et al., 2022
4	La(III)-modified watermelon rind	12.08	308	62.50	Aryal et al., 2022
5	Zr-modified pomegranate peel	8.0	298	72.52	Poudel et al., 2022
6	Zr-chitosan modified Sodium Alginate composite	-	298	43.39	Lou et al., 2021
7	Dried *Chlamydomonas* sp.	4.0	298	53.8	Mohamed et al., 2022
8	Zr (IV)-loaded apple peels	9.0	298	15.68	Mallampati & Valiyaveettil, 2013
9	ZrO_2-coated sawdust	7.0	298	29.0	Setyono & Valiyaveettil, 2014
10	Zr (IV)-modified maize cob (Zr(IV)-MMC)	9.0	298	43.26	This work

Effect of interfering ions

The effect of competitive ions (sulphate, chloride, nitrate, and phosphate) on the sorption of arsenite was analyzed by adding four levels of concentrations of each competitive anion (10, 50, 100, and 200 mg/L) into a 25 mg/L As(III) solution. Competing anions, including sulphate, chloride, nitrate, and phosphate, may compete with arsenite ions for the active site. During adsorption, competing anions such as phosphate, nitrate, chloride, and sulphate may obstruct arsenite ions at the active site. We investigated the adsorption of As(III) oxyanions onto the ideal adsorbent Zr(IV)-MMC when these ions were present. The resultant findings are concisely presented in Figure 7a.

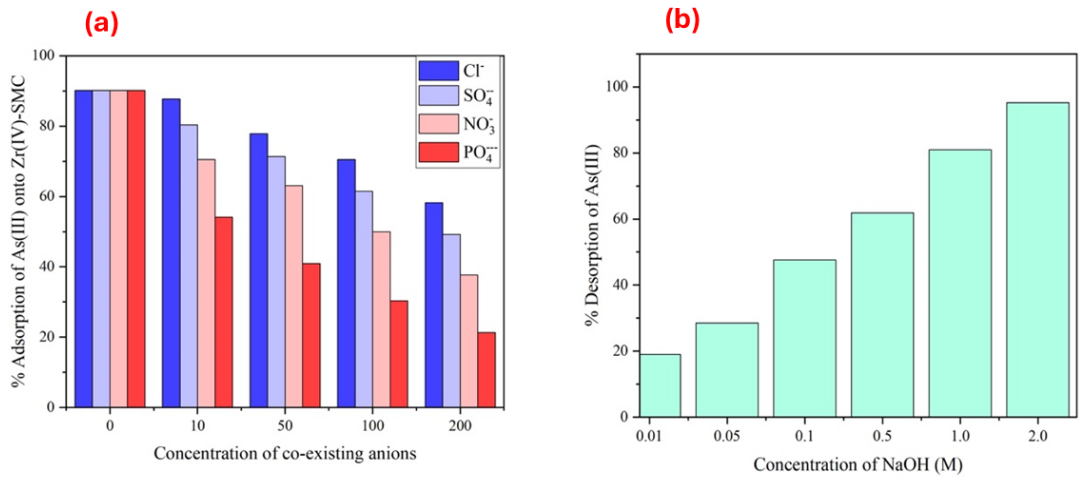

Figure 7. (a) Effect of interfering anions on the adsorptive removal of As(III) by Zr(IV)-MMC (Interfering ions concentration =10, 50, 100 and 200 mg/L), and (b) desorption percentage of As(III) at different NaOH concentrations

These findings demonstrate how other ions might interact with As(III) adsorption, decreasing the adsorbent's removal effectiveness. Among the four tested anions, phosphate showed the highest interference, indicating its higher affinity towards the adsorbent than other anions (Mandal et al., 2013; Aryal et al., 2022).

Desorption of As(III) ions

Generally, NaOH, NaCl or HCl are used as an eluent for the desorption of As(V) (Ghimire, 2003). The interference studies show that Cl^- ion can reduce the adsorption of arsenite. However, the interference from Cl^- was not adequate enough to desorb the arsenite anions, as it has less affinity towards the adsorbent. The highest removal efficiency was achieved at pH 9.0 when assessing the impact of pH on the adsorption process, and the adsorption capacity decreased at pH values above 10. Considering these facts, NaOH was chosen as eluent to desorb the arsenite ions from the Zr(IV)-MMC.

The hydroxyl group replaces the arsenite anion when the arsenite solution is treated with NaOH solution because of the repulsion between the hydroxyl ions and the arsenite anions caused by the pH value rising. As a result, the arsenite anions desorb (Poudel et al., 2022). The results shown in Figure 7b are in excellent agreement with this reasoning, as the increased NaOH concentration from 0.01M to 2M causes desorption of arsenite to reach 95.24%, which proves that Zr(IV)-MMC adsorbent can be regenerated for the next cycle after it reaches saturation.

Inferred mechanism of metal loading and As(III) biosorption/desorption

The NaOH solution is alkaline in nature. When the labile protons of cellulose and lignin that were present in MC were deprotonated in accordance with elementary reaction "a" leaving a negatively charged MC surface where interaction of cationic species of Na^+ is favored via electrostatic attraction, calcium-modified MC (reaction "b"), also known as modified maize cobs and abbreviated as MMC, is produced. During Zr(IV) loading, MMC was treated with $ZrOCl_2 .8H_2O$ at pH 2 to give Zr(IV)-modified MMC [Zr(IV)-MMC]. The loading of Zr^{4+} onto MCB is inferred according to elementary reaction **'c'**.

$$2P{\equiv}OH + NaOH \rightarrow 2\ P{\equiv}O^- + 2H_2O + Na^+ \quad \ldots (a)$$

$$P{\equiv}O^- + Na^+ \rightarrow P{\equiv}ONa \text{ (modified maize cob, MMC)} \quad \ldots (b)$$

$$P{\equiv}ONa + Zr^{4+} \rightarrow P{\equiv}OZr \quad \ldots (C)$$

Here, P: Polymer matrix of maize cob biomass, P≡OH: surface hydroxyl group on maize cob polymer, $P{\equiv}O^-$: deprotonated surface oxygen after alkaline modification, P≡ONa: sodium bound surface oxygen during alkaline treatment, P≡OZr: Zr(IV)-loaded maize cob.

The inferred mechanism for the creation of active sites by loading Zr^{4+} is described as follows. Because of the steric barrier brought on by the massive polymeric structure of cellulose and lignin in MC, it is challenging to neutralize all the positive charges of Zr^{4+} in the loading reaction (Biswas et al., 2008). As a result, the hydroxyl ions in the aqueous medium neutralize the remaining positive charges of Zr^{4+}.

These hydroxyl ligands are substituted during the As(III) biosorption process. Thus, the biosorption of As(III) ions is inferred to occur by replacing the hydroxyl ligand coordinated with Zr^{4+} according to the elementary reaction "d" (Gyawali et al., 2024).

$$P{\equiv}OZr{-}OH + H_2AsO_3^- \rightarrow P{\equiv}OZr{-}H_2AsO_3 + OH^- \quad \ldots (d)$$

$$P{\equiv}OZr{-}H_2AsO_3 + OH^- \rightarrow P{\equiv}OZr{-}OH + H_2AsO_3^- \quad \ldots (e)$$

The exchange of the $H_2AsO_3^-$ ion from As(III)-Zr(IV)-MMC with the hydroxyl ion supplied by the NaOH solution, as shown by reaction "e" is a reasonable explanation for the effectiveness of the NaOH solution in desorbing the adsorbed As(III) anion ($H_2AsO_3^-$).

CONCLUSION

The adsorbent, which was prepared by saponifying raw maize cobs with NaOH and loading them with Zr(IV) at an initial pH of 9.0 (equilibrium pH 9.45), demonstrated the highest adsorption capacity of 43.26 mg/g. The adsorbent was characterized by XRD, FTIR, and SEM-EDX. The biosorption pursued the Langmuir isotherm and PSO kinetic model, showing monolayer chemisorption. Favorability was confirmed by an R_L value between 0 and 1. Among competing ions, phosphate had the most significant interference. The desorption studies indicated that 2M NaOH was the most effective eluent, achieving 95.24% As(III) recovery. All things considered, Zr(IV)-MMC worked better as an adsorbent to remove arsenite from water.

ACKNOWLEDGMENTS

The research facilities provided by the Central Department of Chemistry at Tribhuvan University in Kirtipur, Kathmandu, Nepal, are greatly appreciated by the authors.

AUTHORS CONTRIBUTION

Conceptualization: MRP; Methodology: MRP; Validation: MRP, HP; Investigation: BRP, SD**,** KS**;** Data analysis: DK; Writing-original draft: BRP, SD, KS, DK; Writing-review & editing: HP; Supervision: HP

FUNDING

None

ORCIDs

Bhoj Raj Poudel:
https://orcid.org/0000-0001-7134-5506
Sabin Dhungana:
https://orcid.org/0009-0004-4678-6181
Krishna Subedi:
https://orcid.org/0009-0000-8776-8976
Devendra Khadka:
https://orcid.org/0000-0002-6149-3537
Hari Paudyal:
https://orcid.org/0000-0001-8556-008X
Megh Raj Pokhrel:
https://orcid.org/0000-0003-1148-8753

CONFLICT OF INTEREST

The authors declare that there are no conflicts of interest regarding the publication of this article.

DATA AVAILABILITY STATEMENT

The data supporting the findings of this investigation are accessible from the corresponding author upon reasonable request.

SUPPLEMENTARY INFORMATION

None

REFERENCES

Amin, Md. N., Kaneco, S., Kitagawa, T., Begum, A., Katsumata, H., Suzuki, T., & Ohta, K. (2006). Removal of arsenic in aqueous solutions by adsorption onto waste rice husk. *Industrial & Engineering Chemistry Research*, *45*(24), 8105–8110. https://doi.org/10.1021/ie060344j

American Public Health Association (APHA), American Water Works Association, & Water Environment Federation. (2017). Standard methods for the examination of water and wastewater (23rd ed.). American Public Health Association.

Aryal, M., Ziagova, M., & Liakopoulou-Kyriakides, M. (2010). Study on arsenic biosorption using Fe(III)-treated biomass of *Staphylococcus xylosus*. *Chemical Engineering Journal*, *162*(1), 178–185. https://doi.org/10.1016/j.cej.2010.05.026

Aryal, R. L., Thapa, A., Poudel, B. R., Pokhrel, M. R., Dahal, B., Paudyal, H., & Ghimire, K. N. (2022). Effective biosorption of arsenic from water using La(III) modified carboxyl functionalized watermelon rind. *Arabian Journal of Chemistry*, *15*(3), 103674. https://doi.org/10.1016/j.arabjc.2021.103674

Baig, J. A., Kazi, T. G., Arain, M. B., Afridi, H. I., Kandhro, G. A., Sarfraz, R. A., Jamal, M. K., & Shah, A. Q. (2009). Evaluation of arsenic and other physico-chemical parameters of surface and ground water of Jamshoro, Pakistan. *Journal of Hazardous Materials*, *166*(2), 662–669. https://doi.org/10.1016/j.jhazmat.2008.11.069

Blanchard, G., Maunaye, M., & Martin, G. (1984). Removal of heavy metals from waters by means of natural zeolites. *Water research*, *18*(12), 1501–1507.

Biswas, B. K., Inoue, J. I., Inoue, K., Ghimire, K. N., Harada, H., Ohto, K., & Kawakita, H. (2008). Adsorptive removal of As(V) and As(III) from water by a Zr(IV)-loaded orange waste gel. *Journal of Hazardous Materials*, *154*(1–3), 1066-1074. https://doi.org/10.1016/j.jhazmat.2007.11.030

Chand, T. H., Raj, P. M., Nath, G. K., & Bahadur, K. D. (2015). Removal of arsenic from aqueous solution using iron (III)-modified sugarcane bagasse. *Research Journal of Chemical Sciences, 5(11) 51-58*.

Elizalde-González, M. P., Mattusch, J., & Wennrich, R. (2008). Chemically modified maize cobs waste with enhanced adsorption properties upon methyl orange and arsenic. *Bioresource Technology*, *99*(11), 5134–5139. https://doi.org/10.1016/j.biortech.2007.09.023

Freundlich, H. (1907). Über die adsorption in lösungen. *Zeitschrift für physikalische Chemie*, *57*(1), 385-470.

Ghimire, K. (2003). Adsorptive separation of arsenate and arsenite anions from aqueous medium by using orange waste. *Water Research*, *37*(20), 4945–4953. https://doi.org/10.1016/j.watres.2003.08.029

Gyawali, D., Poudel, M., Gautam, B., Neupane, B. B., Paudyal, H., & Ghimire, K. N. (2024). Zirconium-modified *Citrus limetta* peel for effective removal of arsenic from ground water. *Journal of Water Process Engineering*, *68*, 106283. https://doi.org/10.1016/j.jwpe.2024.106283

Ho, Y. S., & McKay, G. (1998). Sorption of dye from aqueous solution by peat. *Chemical Engineering Journal*, *70*(2), 115–124. https://doi.org/10.1016/S0923-0467(98)00076-1

Lagergren, S. (1898). Zur theorie der sogenannten adsorption geloster stoffe. Kungliga svenska vetenskapsakademiens. *Handlingar* 24, 1-39.

Langmuir, I. (1918). The adsorption of gases on plane surfaces of glass, mica and platinum. *Journal of the American Chemical society*, *40*(9), 1361-1403.

Lin, G., Wang, S., Zhang, L., Hu, T., Peng, J., Cheng, S., & Fu, L. (2018). Synthesis and evaluation of thiosemicarbazide functionalized maizemize bract for selective and efficient adsorption of Au(III) from aqueous solutions. *Journal of Molecular Liquids*, *258*, 235–243. https://doi.org/10.1016/j.molliq.2018.03.030

Lou, S., Liu, B., Qin, Y., Zeng, Y., Zhang, W., & Zhang, L. (2021). Enhanced removal of As(III) and As(V) from water by a novel zirconium-chitosan modified spherical sodium alginate composite. *International Journal of Biological Macromolecules*, *176*, 304–314. https://doi.org/10.1016/j.ijbiomac.2021.02.077

Luo, T., Tian, X., Yang, C., Luo, W., Nie, Y., & Wang, Y. (2017). Polyethylenimine-functionalized maize mize bract, an agricultural waste material, for efficient removal and recovery of Cr(VI) from aqueous solution. *Journal of Agricultural and Food Chemistry*, *65*(33), 7153–7158. https://doi.org/10.1021/acs.jafc.7b02699

Mallampati, R., & Valiyaveettil, S. (2013). Apple peels: A versatile biomass for water purification? *ACS applied materials & interfaces*, *5*(10), 4443–4449. https://doi.org/10.1021/am400901e

Mandal, S., Sahu, M. K., & Patel, R. K. (2013). Adsorption studies of arsenic(III) removal from water by zirconium polyacrylamide hybrid material (ZrPACM-43). *Water Resources and Industry*, *4*, 51–67. https://doi.org/10.1016/j.wri.2013.09.003

Mohamed, M. S., Hozayen, W. G., Alharbi, R. M., & Ibraheem, I. B. M. (2022). Adsorptive recovery of arsenic(III) ions from aqueous solutions using dried *Chlamydomonas* sp. *Heliyon*, *8*(12). https://doi.org/10.1016/j.heliyon.2022.e12398

Montero, J. I. Z., Monteiro, A. S. C., Gontijo, E. S. J., Bueno, C. C., de Moraes, M. A., & Rosa, A. H. (2018). High efficiency removal of As(III) from waters using a new and friendly adsorbent based on sugarcane bagasse and maize cob husk Fe-coated biochars. *Ecotoxicology and Environmental Safety*, *162*, 616–624. https://doi.org/10.1016/j.ecoenv.2018.07.042

Pant, B. D., Adhikari, S., Shrestha, N., Baral, J., Paudyal, H., Ghimire, K. N., ... & Poudel, B. R. (2024). Iron-loaded *Punica granatum* peel: An effective biosorbent for the excision of arsenite from water. *Heliyon*, *10*(17), e37382. https://doi.org/10.1016/j.heliyon.2024.e37382

Paz, R., Viltres, H., Gupta, N. K., Rajput, K., Roy, D. R., Romero-Galarza, A., Biesinger, M. C., & Leyva, C. (2022). Zirconium-organic framework as a novel adsorbent for arsenate remediation from aqueous solutions. *Journal of Molecular Liquids*, *356*, 118957. https://doi.org/10.1016/j.molliq.2022.118957

Poudel, B. R., Ale, D. S., Aryal, R. L., Ghimire, K. N., Gautam, S. K., Paudyal, H., & Pokhrel, M. R. (2022). Zirconium-modified pomegranate peel for efficient removal of arsenite from water. *BIBECHANA*, *19*(1–2), Article 1–2. https://doi.org/10.3126/bibechana.v19i1-2.45943

Poudel, B. R., Aryal, R. L., Gautam, S. K., Ghimire, K. N., Paudyal, H., & Pokhrel, M. R. (2021). Effective remediation of arsenate from contaminated water by zirconium-modified pomegranate peel as an anion exchanger. *Journal of Environmental Chemical Engineering*, *9*(6), 106552. https://doi.org/10.1016/j.jece.2021.106552

Samsuri, A. W., Sadegh-Zadeh, F., & Seh-Bardan, B. J. (2013). Adsorption of As(III) and As(V) by Fe-coated biochars and biochars produced from empty fruit bunch and rice husk. *Journal of Environmental Chemical Engineering*, *1*(4), 981–988. https://doi.org/10.1016/j.jece.2013.08.009

Setyono, D., & Valiyaveettil, S. (2014). Chemically modified sawdust as renewable adsorbent for arsenic removal from water. *ACS Sustainable Chemistry & Engineering*, *2*(12), 2722–2729. https://doi.org/10.1021/sc500458x

Sheng, T., Baig, S. A., Hu, Y., Xue, X., & Xu, X. (2014). Development, characterization and evaluation of iron-coated honeycomb briquette cinders for the removal of As(V) from aqueous solutions. *Arabian Journal of Chemistry*, *7*(1), 27–36. https://doi.org/10.1016/j.arabjc.2013.05.032

Singh, P., Borthakur, A., Singh, R., Bhadouria, R., Singh, V. K., & Devi, P. (2021). A critical review on the research trends and emerging technologies for arsenic decontamination from water. *Groundwater for Sustainable Development*, *14*, 100607. https://doi.org/10.1016/j.gsd.2021.100607

Thapa, S., & Pokhrel, M. R. (2013). Removal of As(III) from aqueous solution using Fe(III) modified pomegranate waste. *Journal of Nepal Chemical Society*, *30*, 29–36. https://doi.org/10.3126/jncs.v30i0.9332

Xu, X., Guo, Q., Yang, C., Hu, Z., Chen, Q., & Hu, J. (2022). Highly effective removal of Hg(II) solution using maizemIZE bract@MoS_2 as a new biomass adsorbent. *RSC Advances*, *12*(49), 31792–31800. https://doi.org/10.1039/D2RA05638K

Yang, M. X., & Zhou, R. (2012). Research on degumming experiment of maizemize bracts. *Advanced Materials Research*, *550–553*, 1242–1247.
https://doi.org/10.4028/www.scientific.net/AMR.550-553.1242

Zong, E., Wei, D., Wan, H., Zheng, S., Xu, Z., & Zhu, D. (2013). Adsorptive removal of phosphate ions from aqueous solution using zirconia-functionalized graphite oxide. *Chemical Engineering Journal*, *221*, 193–203. https://doi.org/10.1016/j.cej.2013.01.088